

Research Paper

Role of matrix metalloproteinase-2/9 (MMP2/9) in lead-induced changes in an *in vitro* blood-brain barrier model

Xinqin Liu^{1*}, Peng Su^{1*}, Shanshan Meng¹, Michael Aschner², Yupeng Cao¹, Wenjing Luo¹, Gang Zheng¹✉, Mingchao Liu¹✉

1. Department of Occupational & Environmental Health and the Ministry of Education Key Lab of Hazard Assessment and Control in Special Operational Environment, School of Public Health, Fourth Military Medical University, Xi'an, 710032, China;
2. Department of Molecular Pharmacology, Albert Einstein College of Medicine, Bronx, NY 10461, USA.

* Xinqin Liu and Peng Su contributed equally to this paper.

✉ Corresponding authors: Dr. Mingchao Liu, Department of Occupational & Environmental Health and the Ministry of Education Key Lab of Hazard Assessment and Control in Special Operational Environment, School of Public Health, Fourth Military Medical University, 169 Changlexi Road, Xi'an, China 710032 Tel: +86 29 84774863 Fax: +86 29 84774862 E-mail: lmclmc@fmmu.edu.cn Or Gang Zheng, E-mail: zhenggang@fmmu.edu.cn

© Ivyspring International Publisher. This is an open access article distributed under the terms of the Creative Commons Attribution (CC BY-NC) license (<https://creativecommons.org/licenses/by-nc/4.0/>). See <http://ivyspring.com/terms> for full terms and conditions.

Received: 2017.04.20; Accepted: 2017.08.16; Published: 2017.10.31

Abstract

Lead (Pb) is a well-known neurotoxicant and a risk factor for neurologic disorders. The blood brain barrier (BBB) plays an important role in the maintenance of optimal brain function. BBB is a target of Pb, and studies have shown that Pb induced barrier loss and decreased the expression of tight junction proteins, but the detailed mechanisms are not fully understood. Matrix metalloproteinases (MMPs) are important components of extracellular matrix proteasome and can affect the remodeling and degradation of tight junction (TJ). The role of MMP-2/9 in Pb-induced damage of BBB is not known. In our study, we used an *in vitro* BBB model by co-culturing human umbilical vascular endothelial cells (ECV304 cells) with rat glioma cells (C6 cells), and detected the expression of related TJ proteins and MMP-2/9. Our results showed that Pb increased the permeability of the *in vitro* BBB model, and stimulating C6 cells with Pb could decrease the protein level of ZO-1 (zonula occludens-1) and occludin in ECV304 cells. Pb could increase the mRNA and protein level of MMP-2/9 in C6 cells, and inhibition of MMP-2/9 by SB-3CT could partially alleviate Pb-induced down-regulation of TJ proteins in ECV304 cells and Pb-induced barrier damage in the *in vitro* BBB model. Our research established potential therapeutic targets for modulating and preserving optimal BBB function.

Key words: Lead; blood brain barrier; matrix metalloproteinase; tight junction.

Introduction

The brain barrier system, including the blood-brain barrier (BBB), blood-cerebrospinal fluid barrier (BCB) and cerebrospinal fluid-brain barrier (CBB), plays a vital role in the maintenance of homeostasis of the central nervous system (CNS). Brain barriers can block the transport of harmful materials from the blood and cerebrospinal fluid barrier (CSF) [1, 2]. BBB is the main component of brain barrier system, and astrocytes are involved in the formation of BBB. Tight junctions (TJs) are fundamental structures in the barrier system. They function as seals and control lateral diffusion between

the apical and basolateral plasma membrane. TJ proteins are primarily made up of occludin, the claudin protein family, occludin, zonula occludens-1 (ZO-1), junctional adhesion molecules (JAM), tricellulin (TRIC) and etc. Decreased TJ protein levels can affect the integrity of the barrier system, leading to the deficits of barrier function.

Lead (Pb) is a ubiquitous environmental heavy metal element. Unlike manganese, copper or iron, Pb had no physiological function and can trigger toxic effects to our bodies. Exposure to excessive Pb can cause multiple toxic effects and induce irreversible

impairments in multiple system, like CNS, urinary system, immune system and etc. Pb poisoning in pregnancy period and childhood can markedly affect the development of neural system, leading to intellectual impairment and cognitive deficits. Although China has prohibited the use of leaded petrol, the pollution of Pb, especially to Pb-induced neurotoxicity, is still a serious situation that must be watched very closely [3]. Pb could affect many structures of CNS, and the brain barrier system is a primary target of Pb [4, 5]. In our previous study, we found Pb could affect the permeability of BBB [6] and BCB [7]. Developmental Pb exposure *in vivo* resulted in BBB impairment, accompanying with decreased levels of tight junction proteins [6, 8]. This effect was mediated, at least in part, by the decreasing of divalent metal transporter 1(DMT1) and iron response element (IRE), as well as intracellular iron levels [6].

Matrix metalloproteinases (MMPs) are important components of extracellular matrix proteasome and affect the remodeling and degradation of extracellular matrix greatly [9]. MMP-2 and MMP-9 express in CNS and have multiple functions. Studies have showed that MMP-2 and MMP-9 could cause the leakage of brain barrier [10], and the mechanism may be mediated by degradation of TJ proteins claudin-5 and occludin [11]. As Pb induced barrier loss and TJ proteins in BBB, we wonder whether MMP-2 and MMP-9 are involved in Pb-induced brain barrier loss.

Our studies mainly aim at investigating the roles of MMP-2 and MMP-9 in lead-induced brain barrier system disorder. The results will provide research basis for the study of Pb-induced neurotoxicity, and provide new ideas for the protective measures.

Materials and Methods

Materials

Analytical pure lead acetate, dexamethasone and fluorescein isothiocyanate dextran (FITC-dextran) were purchased from Sigma (Sigma Chemical Company, St. Louis, MO, USA). Transendothelial electrical resistance (TEER) device was purchased from World Precision Instruments (World Precision Instruments, Berlin, Germany). The inverted microscope and the fluorescence microscope were purchased from Carl Zeiss (Carl Zeiss Meditec, Inc., Dublin, CA). The enzyme-linked immunosorbent spectrophotometer was obtained from Tecan (Männedorf, Switzerland). Transwell devices (Polycarbonate membrane insert, 3.0 μm) were purchased from Costar (Costar, Cambridge, MA, USA). All chemicals were of the highest available purity.

Cell cultures and treatment

C6 glia cells and human umbilical vascular endothelial cells (ECV304) were purchased from Cell Bank of the Chinese Academy of Sciences. These cells were maintained in high-glucose Dulbecco's modified Eagle's medium (DMEM) (Gibco, USA) supplemented with 10% heat-inactivated newborn calf serum (Sijiqing Biotech, China), 100 units/ml of penicillin and 100 $\mu\text{g}/\text{ml}$ of streptomycin in a water-saturated atmosphere of 5% CO₂ at 37 °C. Cells were passaged twice a week.

Lead acetate was dissolved in distilled water at different concentrations, and then freshly diluted with serum-free DMEM to an appropriate concentration. In all analyses, FITC-dextran was dissolved in distilled water at a concentration of 50 mg/ml, then filtered and freshly diluted with serum-free DMEM to an appropriate concentration.

MTT assay

Cell viability was performed to determine the concentration of lead acetate that is optimal for cytotoxicity. Briefly, cells were seeded on 96-well plates at a density of 2×10^4 cells/well. Once confluent, C6 cells or ECV304 cells were treated for 24 h/48 h with graded concentrations of lead acetate (0~100 μM) to determine cell viability. Next, cells were treated with 0.5 mg/ml MTT (dissolved in PBS and filtered through a 0.2- μm membrane) at 37 °C. Four hours later, the formazan crystals were dissolved in DMSO, and the absorption values were determined at 492 nm on an automated Infinite® 200 microplate reader.

In vitro BBB transwell model

Transwell devices were used for the *in vitro* transport studies as previously described [12]. The inner chamber was pre-coated with 0.1% collagen for 4-5 hours in a sterile hood. The *in vitro* BBB model was prepared as reported previously [6, 8]. Briefly, ECV304 cells were added to the inner chamber at a density of 2.0×10^5 cells/ml in 1.0 ml, and C6 cells, at a density of 2.0×10^5 cells/ml were added into 12-well tissue culture plates. The inner chamber containing the ECV304 cells was placed in the 12-well plates with C6 cells and incubated for another indicated growth period (6 d). The 12-well plates contained 1.3 ml of the same medium. The medium was changed every other day after seeding.

To estimate whether Pb-induced barrier function disorder is mediated by ECV304 cells or indirectly by C6 cells, our experiment was divided three groups: control group, in which the *in vitro* BBB model was established without any stimulation; C6+Pb group, in which 10 μM Pb was added into the culture plates and only C6 cells were stimulated by Pb; ECV304+Pb

group, in which 10 μ M Pb was added into the inner chamber and ECV304 cells were stimulated by Pb. The dosage of Pb was confirmed by MTT results and our previous studies [12].

For the tight junction protein study, 10.0×10^5 cells/ml C6 cells, ECV304 cells or C6 cells co-cultured with ECV304 cells were seeded in 3 cm plates, and different dosages of Pb were added into the plates for different periods (6 h ~72 h). After treatment, the medium and the protein were collected and kept in -80 °C. Pb exposure continued until the end of the experiment. The medium was changed every other day after seeding.

Determination of barrier permeability

Transendothelial electrical resistance (TEER) was used to measure the permeability of the *in vitro* BBB model. The methods were performed by manual, and the results were shown as Ohm \times cm², after subtracting the background.

The permeability coefficient (Pe, cm/s) of FITC-dextran (Sigma, Deisenhofen, Germany) was measured and calculated as previously described [13]. After cultured cells were confluent and stimulation were over, the media of the inner chamber were changed with 0.01M PBS+ FITC-dextran (100 μ g/ml, 200 μ l; average molecular mass, 43200; Sigma). At the indicated time points (15, 30, 45, 60 min), 50 μ l of sample medium was taken from the outer chamber. After a dilution of the sample medium to 500 μ l with PBS, the fluorescence intensity of FITC-dextran was measured at excitation and emission wavelengths of 492 nm and 520 nm, respectively, by an automated Infinite® 200 microplate reader. The net value was calculated by subtracting the background value, which was measured on a cell-free chamber (blank).

Western blotting

MMP-2/9 proteins and TJ proteins were detected in C6 cells and ECV304 cells. Cells at 70% confluence were treated with 0, 2.5, 5 and 10 μ M Pb for various time points (6, 12, 24, 48, 72 h). At the end of each treatment, cell lysates were prepared by incubation on ice with lysis buffer, and centrifuged at 20,000 g. The supernatant was collected and protein concentration was determined with the Pierce BCA Protein Assay Kit (Thermo) with bovine serum albumin as a standard control. The supernatant was mixed with equal volume of sample buffer (62.5 mM Tris, pH 6.8, 2% SDS, 5% mercaptoethanol, 1% bromophenol blue, and 25% glycerol). Then the mixture was boiled for 5 min, and centrifuged for 10 min at 10,000 g. The supernatants were used for immunoblotting. Protein extractions were separated by using SDS-PAGE on 10% polyacrylamide gels, and

transferred to nitrocellulose membranes (Millipore, Billerica, MA, USA). After blocking for 1 h with 8% skimmed milk in TBS buffer (10 mM Tris, 150 mM NaCl), the membrane was incubated overnight at 4 °C with primary antibodies, rabbit anti-ZO-1 (1:200, Invitrogen, USA), rabbit anti-occludin (1:200, Invitrogen, USA), rabbit anti-MMP-2 (1:200, Invitrogen, USA), rabbit anti-MMP-9 (1:200, Invitrogen, USA) and mouse anti- β -actin monoclonal antibody (1:1000 dilution, Santa Cruz Biotechnology, CA, USA). Next, the membrane was washed four times for 15 min each with TBST buffer (10 mM Tris, 150 mM NaCl, and 0.1% Tween 20) and incubated at 37 °C for 30 min with the appropriate HRP-conjugated secondary antibody (diluted 1:5000 in TBST). The immuno-positive signal was detected by Fluorchem® FC2 image system (Alpha Innotech, USA). The Fluorchem® FC2 software was used to analyze the gray value of the protein expression in each group. All protein quantifications were adjusted for β -actin levels, which were unchanged by the various treatment conditions.

Quantitative real time (qRT)-polymerase chain reaction (PCR) of TRIC

After treatment, C6 cells or ECV304 cells were rinsed 3 times with PBS, and cell mRNA was isolated with trizol-reagent (Invitrogen, USA). Total RNA was quantified with a NanoDrop ND-100 Spectrophotometer (NanoDrop Technologies, Wilmington, USA). For RT-PCR, primers for the indicated genes and GAPDH were designed with the aid of Clone Manager software and primer sequences were shown in the following table (Table 1). 1 μ g of total RNA was reverse-transcribed into cDNA by using the RNease kit from TakaRa and amplified by PCR reactions. QRT-PCR was performed with SYBR Premix Ex Taq™ Kit (TAKARA) via the applied Biosystem 7500 Fast Real-time PCR System (Applied Biosystem, Madrid, Spain). The sequences for each primer used shown in the following table. Each PCR cycle was composed of denaturing (94°C, 30 s), annealing (30 s), and extension (72°C, 45 s). Annealing temperatures of PCR setting depended on the specific requirement of used primers. The PCR was performed in strips, each sample examined in triplicate and a no-template control was included for each amplification. In order to verify the specificity of the amplification, a melt-curve analysis was performed immediately after the amplification protocol.

Immunofluorescence imaging and TJ protein expression

Cells were washed three times with PBS (pH 7.4) and fixed in absolute methanol for 25 min at 4 °C, and

then permeabilized with 0.05% Triton X-100 for 10 min in ice bath and blocked for 30 min at room temperature with 5% bovine serum albumin (BSA). Next, cells were incubated at 4 °C for overnight with polyclonal anti-ZO-1 (1:200) or monoclonal anti-occludin (1:100), followed by incubation at room temperature for 1 h with Alexa 488 (green)-conjugated anti-rabbit IgG or Alexa 594 (red)-conjugated anti-mouse IgG antibodies (1:1000), and rinsed again with PBS. Cells were examined and photographed with a Carl Zeiss fluorescent microscope. In all studies, blanks were processed as negative controls, except that the primary antibodies were replaced with PBS.

Table 1. Primer sequences

Name	Primer sequences (5'-3')
GAPDH-Q-F	GACAGTCAGCCGCATCTTCT
GAPDH-Q-R	GCGCCCAATACGACCAAATC
MMP-2-Q-F	GCAGCCCATGAGITCGGCCAT
MMP-2-Q-R	AGCATCAGGGGAGGGCCATA
MMP-9-Q-F	GGAGACGGCAAACCTGCGT
MMP-9-Q-R	TGACGTCGGCTCGAGTAGGACA
Occludin-Q-F	TCAGGTGAATTGGTCACCGAG
Occludin-Q-R	GATAAACCAATCTGCTGCGTC
ZO-1-Q-F	TGCCATTACACGGTCCTCTG
ZO-1-Q-R	TCTGCTTCTGTTGAGAGGCT

Statistical analysis

All experiments were performed at least three times, and results were expressed as mean \pm SD. The results were analyzed by one-way analysis of variance (ANOVA) followed by the LSD-t test for multiple comparisons. All analyses were performed with the Statistical Package for the Social Sciences (SPSS 19.0) software. Data were considered statistically significant at p value < 0.05 .

Results

Cell viability of ECV304 cells and C6 cells after Pb treatment

To ascertain the effect of Pb on ECV304 cells and C6 cells, we firstly used MTT assay to detect cell viability. As shown in Fig.1, treatment with different concentrations of Pb in ECV304 cells led to no change in cell viability compared with controls (Fig. 1A). However, $> 25\mu\text{M}$ Pb treatment for 48h reduced C6 cellular viability ($p < 0.05$) (Fig. 1B), and the inhibitory effect was concentration-dependent. As our study aims to investigating the role of Pb in the permeability of barrier without the disruption of cell viability, and combined with our previous study [7], we chose $< 10\mu\text{M}$ Pb as our research dosage.

Effect of Pb on barrier permeability of the *in vitro* BBB model

The results of TEER and the permeability coefficient of FITC-dextran were used to confirm the permeability of *in vitro* BBB model. As shown in Fig. 2A, the values of TEER increased along with time, and the establishment of BBB was started on day 4. Compared with control group, the changes of TEER in ECV304+Pb group were not remarkable, and the differences was too small to be statistically significant. However, the values of TEER in C6+Pb group was much lower than those in control group on day 6 ($p < 0.05$). Fig. 2B showed the fluorescence of FITC dextran and the data were in good consistence with the values of TEER. In control or ECV304+Pb group, the permeability coefficient of FITC-dextran was gradually decreased as the time went by, and the permeability coefficient of FITC-dextran in C6+Pb group was much higher than that in control group on day 4~6 ($p < 0.05$). These data suggest that Pb affects the permeability of the *in vitro* BBB model may be mediated by C6 cells.

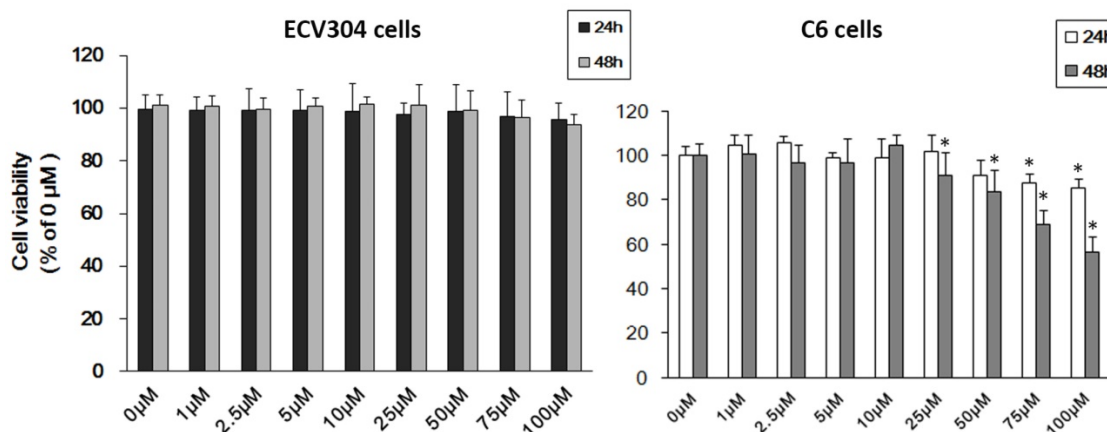


Figure 1. Cell viability of C6 cells and ECV304 cells. (A) Cell viability of ECV304 cells after Pb treatment. (B) Cell viability of C6 cells after Pb treatment. Data are expressed as means \pm SD. * $p < 0.05$ vs. 0 μM .

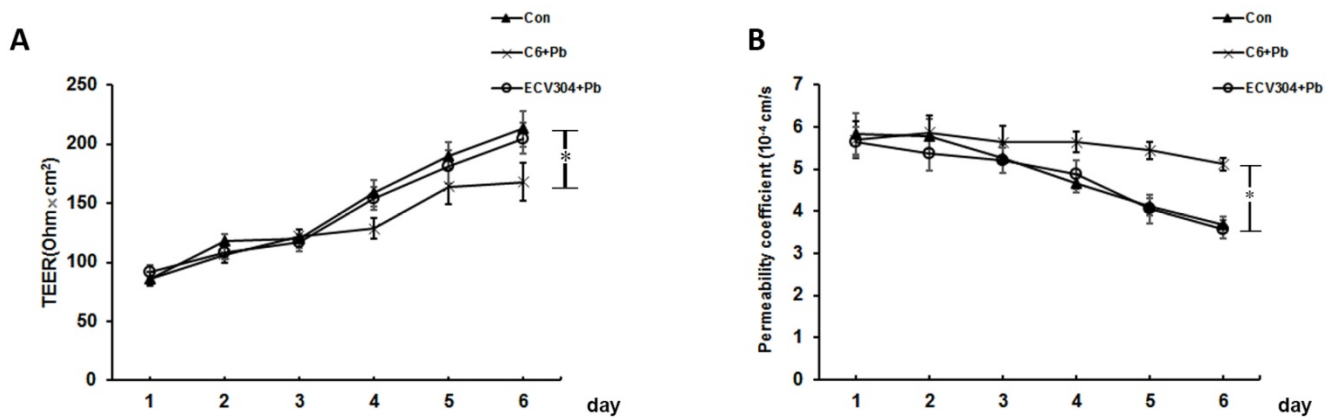


Figure 2. Effect of Pb on barrier permeability of the *in vitro* BBB model. We used C6 cells and ECV304 cells to establish the *in vitro* BBB model. (A) Values of transendothelial electrical resistance (TEER) and (B) Flux of FITC-dextran were assessed in response to control group (Con), ECV304+Pb group and C6+Pb group at different time points. Con group, in which the *in vitro* BBB model was established without any stimulation; C6+Pb group, in which Pb was added into the culture plates and C6 cells were stimulated by Pb; ECV304+Pb group, in which Pb was added into the inner chamber and ECV304 cells were stimulated by Pb. Data represent as means \pm SD (n=3), * p < 0.05 vs. Con.

Effect of Pb on TJ proteins in the *in vitro* BBB model

To determine why Pb could induce barrier leakage mediated by C6 cells, we examined TJ proteins ZO-1 and occludin in the *in vitro* BBB model. As shown in Fig. 3A, different dosages (0, 5, 10 μ M) of Pb were used to investigate TJ proteins with or without C6 cells, and the results displayed that treatment with different concentrations of Pb (0, 5, 10 μ M) for 48 h had no effect on occludin and ZO-1 protein expression in ECV304 cells without C6 cells. However, ECV304 cells co-cultured with C6 cells treated with Pb for 48h significantly down-regulated occludin and ZO-1 protein levels in a concentration-dependent manner (Fig. 3A and 3B). To further confirm our results, we also assessed TJ protein levels upon C6 cells+Pb treatments at different time points (24 h ~72 h) (Fig. 3C and 3D), and the data of western blot showed that C6 cells+Pb reduced ZO-1 protein levels at 48 h and 72 h (Fig. 3C and 3D), and >5 μ M Pb inhibited the expression of ZO-1 and >2.5 μ M Pb in occludin (p <0.05) (Fig. 3D).

To confirm the results of protein level, immunofluorescence staining was carried out. Fig. 4A and 4B showed that the expression of occludin or ZO-1 in ECV304 cells was reduced after treatment with C6 cells +Pb, compared with ECV304 cells cocultured with C6 cells. In the *in vitro* BBB model, the expression of occludin or ZO-1 was displayed as continuous network distributed in the intercellular space. Pb treatment reduced the immunofluorescence density of occludin or ZO-1 (p <0.05), but also disrupted the integrity of TJ proteins. Taken together, these data establish that treatment with C6 cells may release some components, which lead to the dysfunction of the *in vitro* BBB barrier.

Effect of Pb on the expression of MMP-2/9 in the *in vitro* BBB model

Previous studies have shown that the expression of MMP-2/9 affected tight junctions and basement membrane proteins [14]. To test whether Pb-induced the expression of MMP in C6 cells led to barrier-loss in the *in vitro* BBB model, we investigated the expression of MMP-2/9 by qRT-PCR and western blot analysis in C6 cells. Fig. 5A shows mRNA level of MMP-2/9 in C6 cells after treatment with Pb for 6 h ~48 h. The results showed that MMP-2/9 mRNA levels did not change at 6h, and MMP-2 concentration-dependently was upregulated at 12 h and 24 h; mRNA levels of MMP-9 increased after Pb treatment for 24 h. However, the level of MMP-2/9 was restored to the normal level at 48h (Fig. 5A). Next, we investigated the protein expression of MMP-2/9 in C6 cells, and found that after treatment with Pb for 6 h, the protein level of MMP-2 was transiently upregulated at 5 and 10 μ M Pb treatment. The MMP-2 level returned to the normal level at 12 h, but upregulated at 24 h and 48 h (Fig. 5B and 5C). The protein expression of MMP-9 was markedly increased at 24 h and 48 h compared with the 0 μ M group (p <0.05) (Fig. 5D). These data suggest that Pb induces predominantly the up-regulation of MMP-2/9.

Effect of Pb on the barrier function after inhibition of MMP-2/9

To further confirm the effects of MMP-2, an MMP-2/9 inhibitor SB-3CT was used to inhibit the expression of MMP-2/9. In order to choose a suitable concentration, we firstly used different concentrations of SB-3CT to detect cell viability of C6 cells via MTT assay. As shown in Fig 6A, >50 μ M SB-3CT inhibited cell viability, thus we selected 30 μ M SB-3CT. Next,

we assessed TJ proteins expression in the *in vitro* BBB model, noting that SB-3CT alone had no significant effect on the expression of TJ protein, but pretreatment SB-3CT could alleviate the down-regulation of ZO-1 and occludin induced by Pb exposure (Fig. 6B and 6C). mRNA levels of MMP-2 and MMP-9 were testified after treatment with SB-3CT in C6 cells, and the results showed that 30 μ M SB-3CT effectively decreased the mRNA levels of MMP-2 and MMP-9 (Fig. 6D). To further investigate

the role of SB-3CT on the barrier function, TEER and the permeability coefficient of FITC-dextran were testified. Compared with control group, the values of TEER in Pb group and SB-3CT+Pb were reduced, but SB-3CT treatment could partially reverse the harmful effect of Pb exposure (Fig. 6E), and results of FITC-dextran results were in good consistence with results of TEER (Fig. 6F). These data suggest that inhibition of MMP-2/9 can mitigate Pb-induced increased permeability of the *in vitro* BBB.

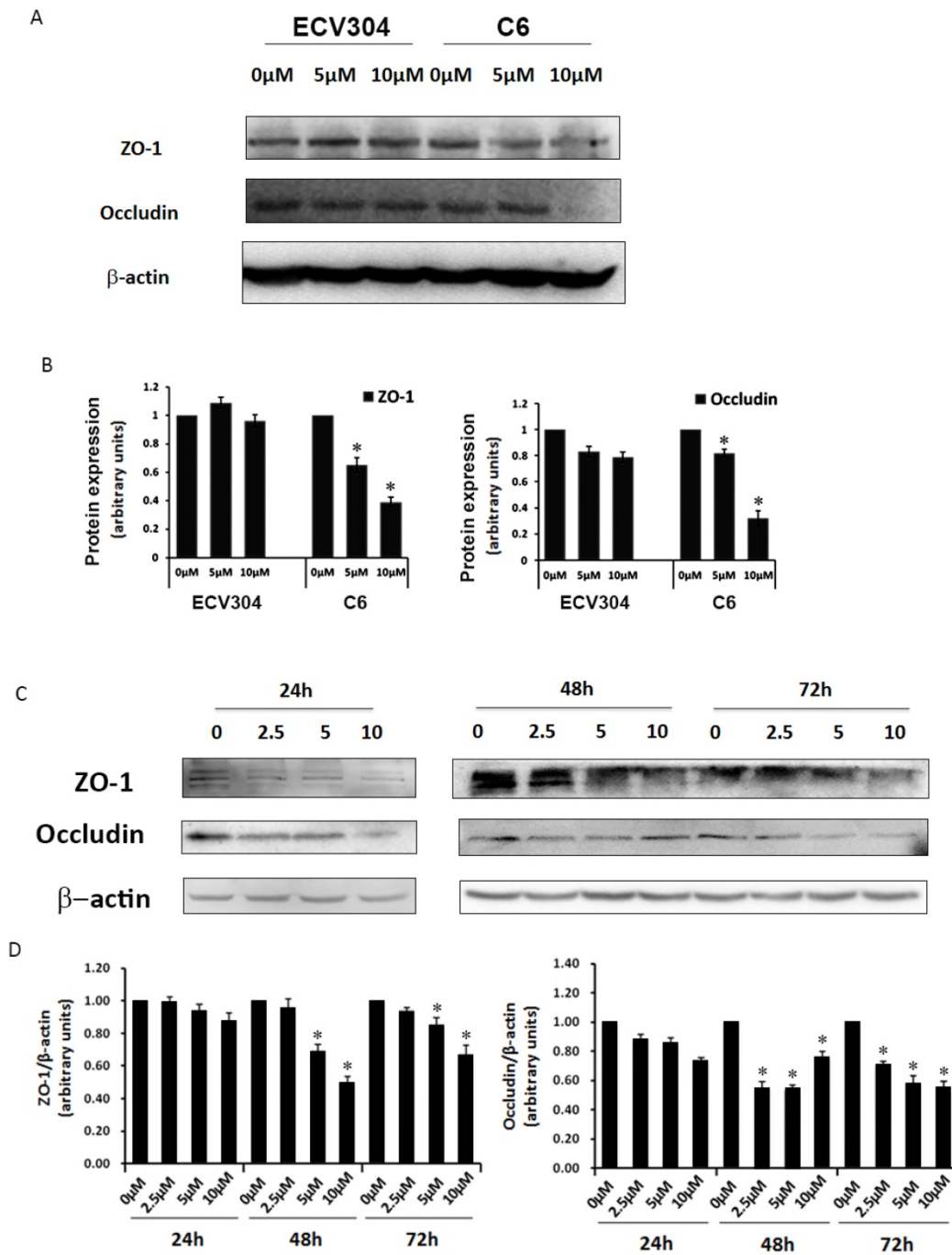


Figure 3. Expression of TJ proteins in response to different treatments. (A) Protein expression of ZO-1 and occludin in ECV304 cells. ECV304 cells or C6 cells co-cultured with ECV304 cells were seeded in plates, and different concentrations of Pb was add into the medium for 48h. (B) Gray analysis of TJ proteins level. (C) Protein expression of ZO-1 and occludin in response to Pb treatment with different time points in C6 cells co-cultured with ECV304 cells. (D) Gray analysis of TJ proteins level, and data are shown as means \pm SD, * p < 0.05 vs. 0 μ M.

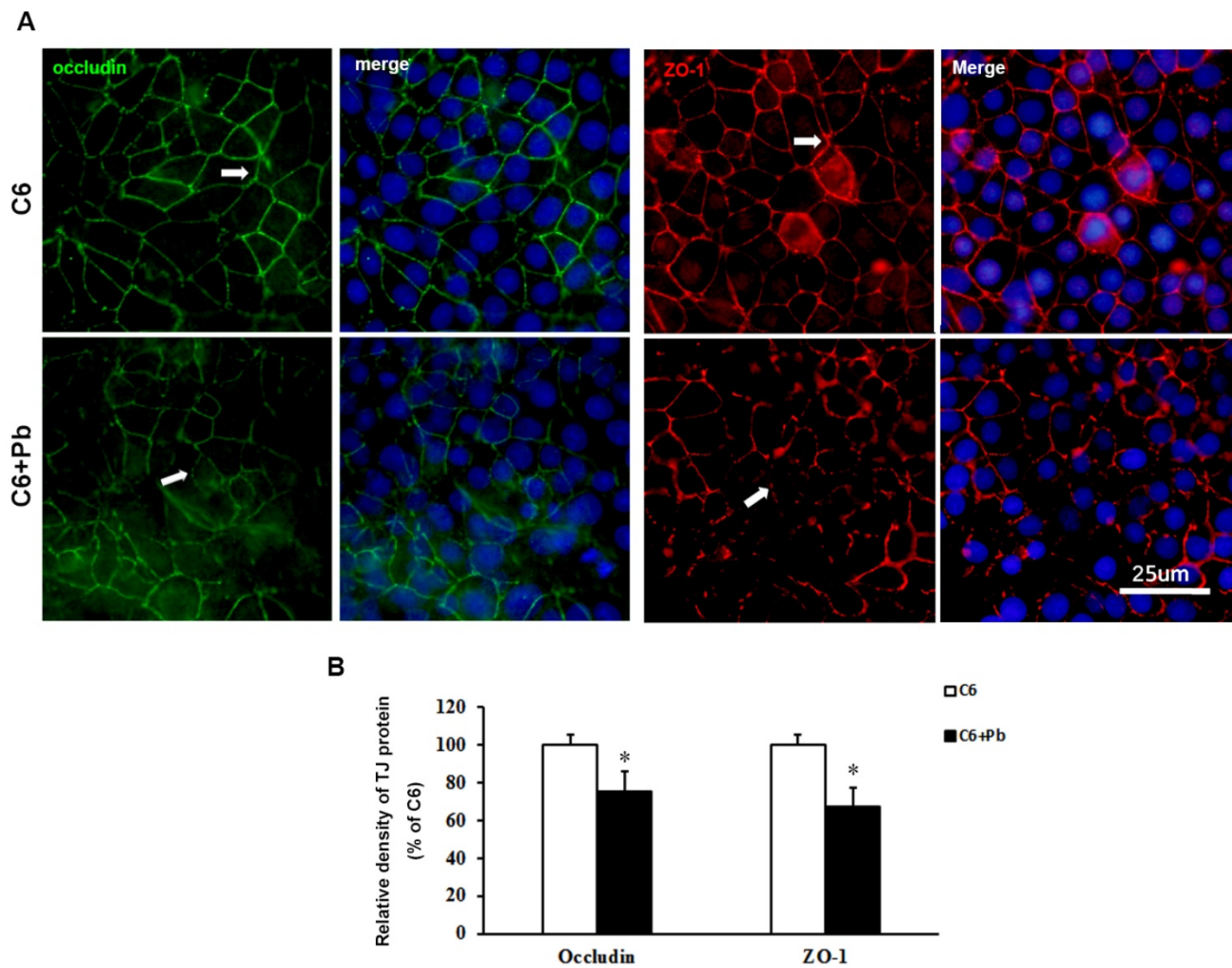


Figure 4. Immunofluorescence images of TJ proteins. C6 cells co-cultured with ECV304 cells to establish the *in vitro* BBB model, and Pb was added to the medium for 48 h. (A) Immunofluorescence images for occludin (green) and hoechst (blue) or for ZO-1 (red) and hoechst (blue), scale bar= 25 μ m. C6 group: C6 cells co-cultured with ECV304 cells without stimulation, C6+Pb group: C6 cells co-cultured with ECV304 cells with 10 μ M Pb. The white arrows represent the distribution of TJ proteins. (B) Relative density of TJ protein. Data are shown as means \pm SD, * p < 0.05 vs. C6 group.

Discussion

Great attention has been paid to Pb-induced neurotoxicity and the prevention of Pb pollution [15]. Brain barrier system, as the first line of defense system in the CNS, can prevent lots of external components but can't prevent Pb. Our previous studies showed that Pb could interfere with optimal BBB development and integrity, and the mechanism may be mediated by DMT1 [6, 8]. In another study, Pb could affect the expression of TJ proteins [16]. Previous studies suggested that Pb could entrance into brain parenchyma in multiple ways. As we know, BBB is made up of brain microvascular endothelial cells and astrocytes, and the function of astrocyte play an important role in maintenance of barrier function. In our present study, we found that Pb-induced BBB leakage may be mediated by MMP-2/9 released by astrocytes, and MMP-2/9 induced by Pb could

degraded the TJ proteins occludin and ZO-1 between adjacent endothelial cells, and destroyed the integrity of barrier.

Pb pollution is a worldwide health problem. In China, although the government has forbidden the usage of leaded petrol, the pollution of Pb is still a serious problem. With the increasing awareness of prevention, the incidence of acute Pb toxicity and occupational Pb toxicity are gradually declining, but that of chronic Pb toxicity and low concentration Pb toxicity are increasing. Studies have shown that even relative low dosage of Pb exposure could induce neurotoxicity [17]. Therefore, our research aims at the effect of low-dosage Pb exposure on the function of BBB. Since the BBB is mainly made up of brain microvascular endothelial cells and astrocyte, we first established an *in vitro* model using ECV304 and C6 astrocytic cells. And MTT assay was used to choose a suitable concentration, in which Pb could not affect

the viability of cells. In our study, we found that < 10µM Pb had no effect on cell viability (Fig. 1), but could induce barrier function disorders (Fig. 2), so we

assumed that low dosage of Pb's toxic effect may be mediated by astrocytes, not directly by endothelial cells.

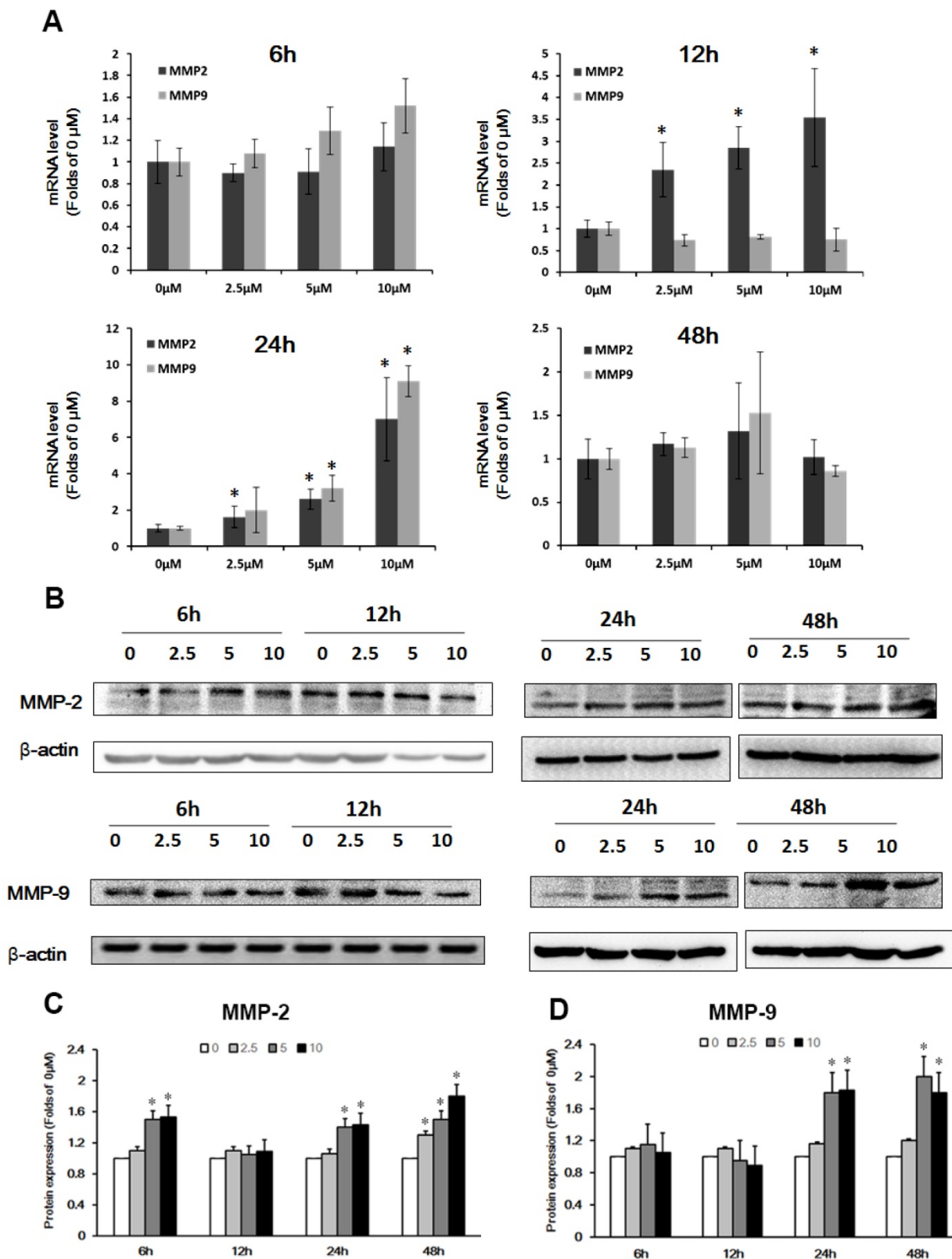


Figure 5. Effect of Pb treatment on MMP-2/9 in C6 cells. (A) The mRNA expression of MMP-2 and MMP-9 after treatment with different dosages of Pb in C6 cells. (B) The protein expression of MMP-2 and MMP-9 after treatment with different dosages of Pb in C6 cells. (C) and (D) Gray analysis of MMP-2 and MMP-9 protein level. Data are expressed as means ± SD (n=3), * p < 0.05 vs. 0 µM.

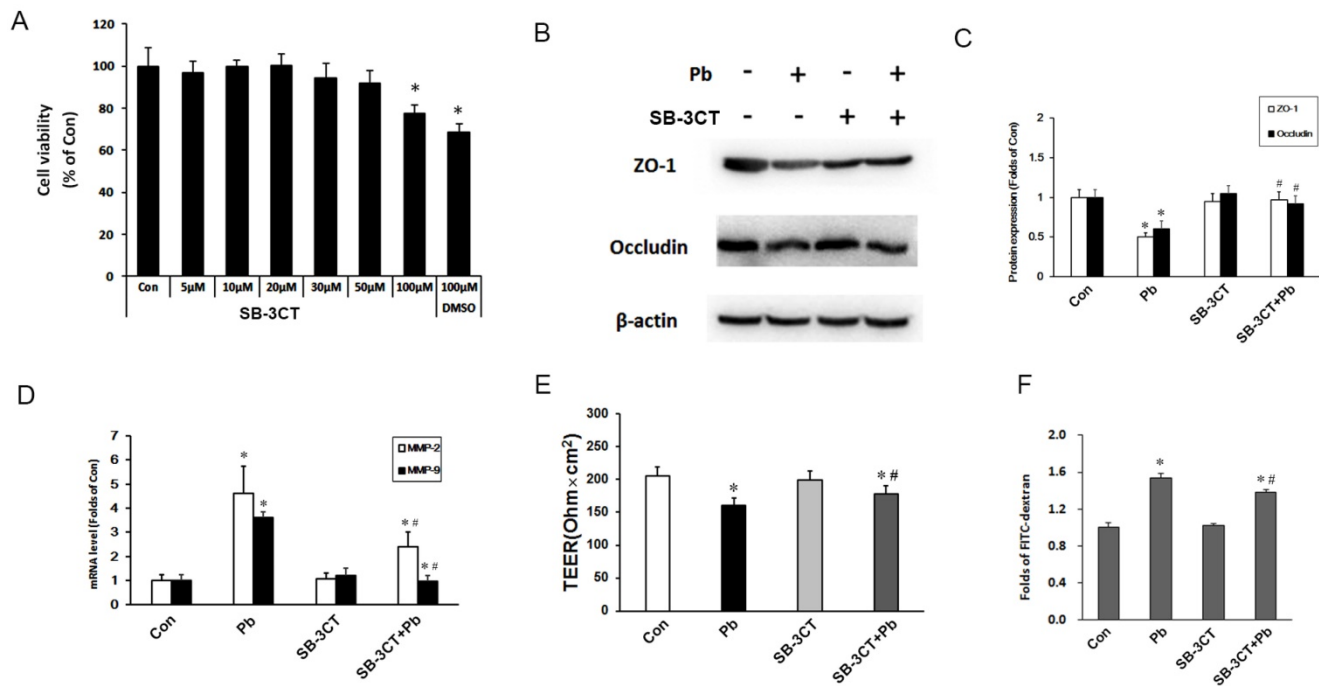


Figure 6. Determination of the *in vitro* BBB barrier permeability after inhibition of MMP-2/9. (A) Cell viability of C6 cells after treatment with SB-3CT in response to Pb exposure. (B) Protein level of MMP-2/9 in response to SB-3CT or Pb in abovementioned C6 + ECV304 cells co-culture system, and Pb or SB-3CT were added in the medium of C6 cells. (C) Gray analysis of MMP-2/9 protein level. Data are expressed as the means \pm SD ($n=3$), * $p < 0.05$ vs. control. (D) mRNA level MMP-2/9 in response to SB-3CT or Pb. (E) Data of TEER and (F) flux of FITC-dextran flux. Data are expressed as means \pm SD ($n=3$), * $p < 0.05$ vs. con, # $p < 0.05$ vs. Pb.

To confirm our assumption, Pb was added into the medium of ECV304 cells or C6 cells, and the results showed that only Pb treatment with C6 cells could affect the expression of TJ proteins in the *in vitro* BBB model, and the effect of Pb was time-dependent and dosage-dependent (Fig. 3). Data of immunofluorescence images also showed low expression of TJ proteins in C6+ Pb, corroborating the protein data (Fig. 4). These results suggested that astrocytes treatment with Pb led to the release of some component which could affect the expression and distribution of TJ proteins.

MMPs participate in many physiology and pathological processes in the brain and at BBB [18]. Previous research had shown that MMPs degrade TJ proteins and basement membrane proteins, although there was little data to support this *in vivo*, which may be limited to the technical problem. Gu et al showed that MMP activity was increased and barrier permeability at the BBB was higher in stroke during reperfusion *in vivo* [19]. Another study showed increased MMP-2 and MMP-9 mRNA and activity levels after reperfusion in spontaneously hypertensive rats with middle cerebral artery occlusion (MCAO), and the permeability of BBB in the cortex was increased upon the disruption of TJ proteins [20], strongly implying MMPs-mediated tight junctions disruption. Pb could affect the expression of MMP-2, MMP-9 and TIMP-2 [21-23] in

epithelial cells and endothelial cells, but the mechanism remains unclear. Given the previous studies, we wondered whether Pb induced the expression of MMPs in astrocytes, leading to the degradation of TJ proteins. Our results showed that Pb significantly increased MMP-2/9 mRNA levels and protein levels in C6 cells (Fig. 5), which suggested that MMP-2/9 may effect on barrier function of BBB. Pb could affect the function of astrocytes by multiple pathways. Previous studies showed that astrocytes could act as Pb accumulation pools in the brain through enhance the levels of GRP78 in astrocyte endoplasmic reticulum [24], and up-regulation of GRP78 could increase the expression of MMP-2, MMP-9 and TIMP-1[25], which may be the underlying mechanism of Pb-induced upregulation of MMP-2/9 in astrocytes.

To confirm the role of MMP-2/9, we used SB-3CT, an MMP-2/9 inhibitor, to reduce the expression of MMP-2/9. The data of qRT-PCR and western blot suggested that inhibition MMP-2/9 partially reversed the down-regulation of TJ proteins in ECV304 cells (Fig. 6). The results of TEER and FITC-dextran also showed that ECV304 cells treated with SB-3CT, at least in part, diminished the leakage of the *in vitro* BBB.

Taken together, our results showed that Pb increased the expression of MMP-2 and MMP-9 in astrocytes and the release of MMP-2/9 degraded TJ

proteins in brain microvascular endothelial cells, leading to the increased barrier permeability. What's more, inhibition of MMP-2/9 could significantly alleviate the harmful effect of Pb on BBB. Therefore, our research establishes potential new therapeutic targets for modulating and preserving optimal BBB function.

Abbreviations

Pb, lead; TJ, tight junction; BBB, blood brain barrier; BCB, blood-cerebrospinal fluid barrier; ZO-1, zonula occludens-1; TEER, transendothelial electrical resistance; FITC, fluorescein isothiocyanate; JAM, junctional adhesion molecules; MMP-2/9, matrix metalloproteinase-2/9

Acknowledgements

This work was supported by National Basic Research Program of China (973 Program, 2012CB525004); National Key Technology Support Program (2014BAI12B04); Key Project of Natural Science Foundation of China (81472942, 81230063); Program for Changjiang Scholars (T2011153) and Innovative Research Team in University (PCSIRT); Young Elite Project of Fourth Military Medical University; Program for New Century Excellent Talents in University. Michael Aschner was supported in art by NIH grants, R01 ES10563, R01 ES10563S1 and R01 ES07331.

Competing Interests

The authors have declared that no competing interest exists.

References

- Schneeberger EE, Lynch RD. The tight junction: a multifunctional complex. *Am J Physiol Cell Physiol* 2004;286:C1213-C1228
- Tsukita S, Furuse M, Itoh M. Multifunctional strands in tight junctions. *Nat Rev Mol Cell Biol* 2001;2:285-293
- Li MM, Cao J, Xu J, et al. The national trend of blood lead levels among Chinese children aged 0-18 years old, 1990-2012. *Environ Int* 2014;71:109-117
- Liu KS, Hao JH, Zeng Y, Dai FC, Gu PQ. Neurotoxicity and biomarkers of lead exposure: a review. *Chin Med Sci J* 2013;28:178-188
- Baranowska-Bosiacka I, Gutowska I, Rybicka M, Nowacki P, Chlubek D. Neurotoxicity of lead. Hypothetical molecular mechanisms of synaptic function disorders. *Neurol Neurochir Pol* 2012;46:569-578
- Wang Q, Luo W, Zhang W, et al. Involvement of DMT1 +IRE in the transport of lead in an in vitro BBB model. *Toxicol in Vitro* 2011;25:991-998
- Su P, Zhao F, Cao Z, et al. Mir-203-mediated tricellulin mediates lead-induced in vitro loss of blood-cerebrospinal fluid barrier (BCB) function. *Toxicol in Vitro* 2015;29:1185-1194
- Wang Q, Lin Y, Zhang W, et al. Lead induces dysregulation of iron regulatory protein 1 via the extracellular signal-regulated kinase pathway in human vascular endothelial cells. *Brain Res* 2012;1455:19-27
- Abdul MP, Alikunju S, Szlachetka AM, Murrin LC, Haorah J. Impairment of brain endothelial glucose transporter by methamphetamine causes blood-brain barrier dysfunction. *Mol Neurodegener* 2011;6:23
- Visse R, Nagase H. Matrix metalloproteinases and tissue inhibitors of metalloproteinases: structure, function, and biochemistry. *Circ Res* 2003;92:827-839
- Zhang YM, Zhou Y, Qiu LB, Ding GR, Pang XF. Altered expression of matrix metalloproteinases and tight junction proteins in rats following PEMP-induced BBB permeability change. *Biomed Environ Sci* 2012;25:197-202

- Shi LZ, Li GJ, Wang S, Zheng W. Use of Z310 cells as an in vitro blood-cerebrospinal fluid barrier model: tight junction proteins and transport properties. *Toxicol in Vitro* 2008;22:190-199
- Yeh WL, Lu DY, Lin CJ, Liou HC, Fu WM. Inhibition of hypoxia-induced increase of blood-brain barrier permeability by YC-1 through the antagonism of HIF-1 α accumulation and VEGF expression. *Mol Pharmacol* 2007;72:440-449
- Rempe RG, Hartz AM, Bauer B. Matrix metalloproteinases in the brain and blood - brain barrier: versatile breakers and makers. *Journal of Cerebral Blood Flow & Metabolism* 2016;:271678X-1665551X
- Lopes AC, Peixe TS, Mesas AE, Paoliello MM. Lead Exposure and Oxidative Stress: A Systematic Review. *Rev Environ Contam Toxicol* 2016;236:193-238
- Wang Q, Luo W, Zhang W, et al. Iron supplementation protects against lead-induced apoptosis through MAPK pathway in weanling rat cortex. *Neurotoxicology* 2007;28:850-859
- Su P, Zhang J, Wang S, et al. Genistein alleviates lead-induced neurotoxicity in vitro and in vivo: Involvement of multiple signaling pathways. *Neurotoxicology* 2016;53:153-164
- Feng S, Cen J, Huang Y, et al. Matrix metalloproteinase-2 and -9 secreted by leukemic cells increase the permeability of blood-brain barrier by disrupting tight junction proteins. *Plos One* 2011;6:e20599
- Gu Y, Zheng G, Xu M, et al. Caveolin-1 regulates nitric oxide-mediated matrix metalloproteinases activity and blood-brain barrier permeability in focal cerebral ischemia and reperfusion injury. *J Neurochem* 2012;120:147-156
- Yang Y, Estrada EY, Thompson JF, Liu W, Rosenberg GA. Matrix metalloproteinase-mediated disruption of tight junction proteins in cerebral vessels is reversed by synthetic matrix metalloproteinase inhibitor in focal ischemia in rat. *J Cereb Blood Flow Metab* 2007;27:697-709
- Chen L, Yang X, Jiao H, Zhao B. Tea catechins protect against lead-induced ROS formation, mitochondrial dysfunction, and calcium dysregulation in PC12 cells. *Chem Res Toxicol* 2003;16:1155-1161
- Gonzalez-Puebla E, Gonzalez-Horta C, Infante-Ramirez R, et al. Altered expressions of MMP-2, MMP-9, and TIMP-2 in placentas from women exposed to lead. *Hum Exp Toxicol* 2012;31:662-670
- Lahat N, Shapiro S, Froom P, et al. Inorganic lead enhances cytokine-induced elevation of matrix metalloproteinase MMP-9 expression in glial cells. *J Neuroimmunol* 2002;132:123-128
- White LD, Cory-Slechta DA, Gilbert ME, et al. New and evolving concepts in the neurotoxicology of lead. *Toxicol Appl Pharmacol* 2007;225:1-27
- Yuan XP, Dong M, Li X, Zhou JP. GRP78 promotes the invasion of pancreatic cancer cells by FAK and JNK. *Mol Cell Biochem* 2015;398:55-62